Design and Implementation of Dolph Chebyshev and Zolotarev Circular Antenna Array

K. N. Mohan[1], D. Kannadassan[1*] and S. R. Zinka[2]

[1]School of Electronics Engineering, VIT University, Vellore - 632014, Tamil Nadu, India; mohan.kn@vit.ac.in,
dkannadassan@vit.ac.in
[2]BITS Pilani, Hyderabad - 500078, Telangana, India; srinivas.zinka@vit.ac.in

Abstract

Objectives: Uniform Circular Antenna arrays (UCAs) are most common in conformal antenna arrays with uniform excitation of elements. We targeted to design and synthesis UCAs with a high gain of >10 dB and a low sidelobe level of <20 dB. **Methods:** In this paper, the Uniform Circular Array (UCA) is presented with phase mode theory to extract the mode excitation using newly developed ARRAYTOOL. Along with phase modes, the magnitude distribution of elements is synthesized with Chebyshev and Zolotarev Polynomials whose resulting far-field patterns are desirable. **Findings:** It is observed that the Chebyshev and Zolotarev far-field pattern results a low sidelobe of 20 to 25 dB with fewer elements. It's also observed that the elements spacing of more than $\lambda/4$ yields grating lobes with the visible region. This is one the design constrains for UCA with non-uniform excitation. **Improvements:** In comparison with uniformly excited UCAs, the Chebyshev and Zolotarev Polynomials show desirable radiation patterns with fewer elements. With sidelobe of less than 25 dB and minimum null points, the proposed microstrip array shows expected performance for RADAR system with high rotational symmetry.

Keywords: Antenna Array Factor, Dolph Chebyshev, HPBW, Uniform Circular Array

1. Introduction

Uniform Circular Array (UCA) has many potential applications in advanced wireless technology such as smart phones, RADAR and satellite[1,2]. While comparing other linear or planar arrays, UCAs are beneficial as they have flexible and symmetric radiation patterns[3], full azimuth scan capability[4,5], nearly Omni-directional[6] and conformal to the surface. These capabilities are useful in target prediction in recent wireless technologies such as spatial MIMO, beam forming sensor and mesh networking. In this regard, few works have been carried out to optimize the radiation pattern of UCAs with non-uniform excitation of elements[7], beam-forming[8] and evolutionary algorithms of optimization[9,10]. Along with target prediction, interference cancellation is a challenging task for such transceivers which needs UCAs with high directivity and desired Side Lobe Level (SLL) together. This is possible by introducing non-uniform excitation, such as in distribution in UCAs. Phase mode theory was successful

in computation of current distributions for UCA using a phasing transformation on linear array[11–17]. Our group has demonstrated the numerical simulation of circular array using phase mode excitation through ARRAY TOOL[18–20]. Phase mode excitation in UCAs is beneficial in many ways. Phase modes are orthogonal since its transformed using Fourier series, so they do not have mutual coupling. Also the shape of the radiation pattern is independent of frequency since $kdsin\theta$ plane of linear array transformed to θ plane. In[21] it is observed that shape of the radiation pattern not affected by number of elements. According to phase mode theory, beam patterns of UCAs are naturally formed with Bessel function which results many side lobes of unequal amplitude. As concentration of elements in circular array increases, beam width is reduces drastically than that of linear array. It is observed that the number of side-lobes can be reduced by symmetrical amplitude taper on the front half of the circular array low excitation on the back of the array[22]. It is clear that a directional radiation pattern can be easily synthesized using UCA

by addressing either special harmonics or phase mode excitations. However, excitation of nth mode/harmonic needs appropriate multi-port feeding network. On the other hand, the continuously varying phase component of each element can be corrected by tapering the array with phase, referred as phase compensated circular array. This yield a beam with all elements is in phase. Directional radiation pattern in UCA with low sidelobe can be implemented by introducing directional antennas/elements. In have demonstrated the first of its kind with unidirectional elements with semi-circular phase compensated array. With element spacing of 0.45λ, a low side-lobe level of 20 dB achieved with amplitude tapering. Implementation of amplitude tapering or non-uniform excitation with polynomials is efficient method and challenging task. A. T. Villeneuve has developed a synthesis technique for discrete circular array by combining uniform and Dolph Chebyshev (D-C) excitations[23]. In this method, the pattern synthesis is initiated with uniform excitation and replacing them by first $n-1$ modified D-C roots. Villeneuve's method results beam pattern same as Taylor beam pattern. Recently, the synthesis and computational techniques of current distribution for D-C patterns for circular arrays were demonstrated by in[24]. In most of the studies, the synthesis of UCAs is demonstrated with isotropic elements. In practical systems, directional elements of UCAs will largely impact on side-lobe levels. In this paper, we have demonstrated the implementation of UCA with D-C and Zolotarev excitation with directional element as circular/rectangular patches. With phase's mode excitation, the UCAs are synthesized with uniform and D-C, Zolotarev excitations. Incorporation of directional elements with phase mode excitations is demonstrated. The EM simulation and theoretical computations are compared in various principle planes. From the results obtained, the uniform spacing of circular ring array provides the desired sidelobe level of different polynomials is applied to the uniform excitation far field. The results taken into literature and it are useful analytical model for wireless communication.

2. Phase Mode Excitation of Dolph-Chebyshev UCAs

2.1 Pattern Analysis

In circular discrete arrays, the Omni-directional patterns are expressed in terms of spatially orthogonal phase

modes. In treated the phase modes as similar to that of uniformly spaced linear array. In general, the radiation pattern of UCAs with radially disposed radiating elements cannot be separated into array-factor and element-patterns directly. Instead, each element pattern should be included into the total radiation pattern. Figure 1 shows the continuous and radially disposed circular ring array. And the radiated farfield pattern is given as,

$$F(\theta,\phi) = R_o \int_0^{2\pi} (A(\beta) \, G_e(\theta, \phi - \beta) \, e^{(jk_o R_o \sin\theta \cos(\phi - \beta))}) \, d\beta \tag{1}$$

Where R_o is the radius of the ring, $A(\beta)$ and $G_e(\theta, \phi - \beta_n)$ are aperture excitation and element pattern respectively. β is the phase factor with respect to the origin. For discrete circular ring arrays, aperture excitation can be expressed as $A(\beta) = A^n(\beta) = \sum_{n=1}^{N} A^d_n \delta(\beta - \beta_n)$. Therefore the Equation (1) can be rewritten as

$$F(\theta,\phi) = R_o \sum_{n=1}^{N} A^d_n G_e(\theta, \phi - \beta)e^{jk_o R_o \sin\theta \cos(\phi - \beta_n)} \tag{2}$$

Since $A(\beta)$ is a periodic function with period of 2π, the ring source distribution can be written as Fourier series,

$$A(\beta) = \sum_{m=-\alpha}^{\alpha} a_m e^{jm\beta} \tag{3}$$

Where

$$a_m = \frac{1}{2\pi} \int_0^{2\pi} A(\beta) e^{-jm\beta} \, d\beta \tag{4}$$
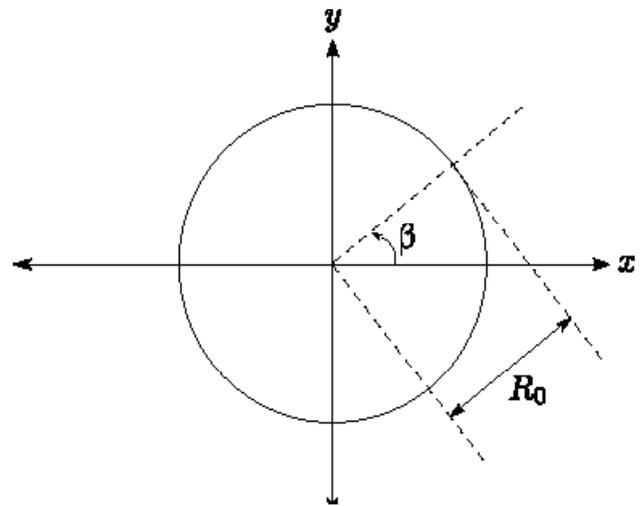
For discrete arrays, the above equation becomes

Figure 1. Continues circular ring source.

$$a_m = \frac{1}{2\pi \sum_{n=1}^{N} A^d{}_n e^{-jm\beta_n}} \tag{5}$$

This result

$$a_m \int_0^{2\pi} F(\theta,\phi) = R_0 \sum_{m=-\alpha}^{\alpha} a_m e^{jm\beta} G_e(\theta,\phi-\beta)$$

$$e^{jk_oR_o\sin\theta\,\cos(\phi-\beta)} e^{-jm\beta} d\beta \tag{6}$$

For a given azimuthal θ, element pattern $G_1e\,(\theta,\phi\,)$ also can be written in terms of a Fourier series as shown.

$$G_e(\theta,\phi) = \sum_{p=-\alpha}^{\alpha} g_p(\theta) e^{jl\phi} \tag{7}$$

Where,

$$g_p(\theta) = \frac{1}{2\pi} \int_0^{2\pi} G_e(\theta,\phi) e^{-jl\phi} d\phi \tag{8}$$

From Equation (7), the discrete form can be expressed, along with β as,

$$G_1e\,[\theta,(\phi-\beta) = \Sigma_1(p=-\alpha)^\dagger\alpha \boxtimes \square g_1p\,(\theta)\,e^\uparrow jl(\phi-\beta) \tag{9}$$

By substituting the Equation (9) in Equation (6), we get,

$$F(\theta,\phi) = R_o a_m \sum_{p=-\alpha}^{\alpha} g_p(\theta) e^{jl\phi} \int_0^{2\pi} e^{jk_oR_o\sin\theta\,\cos(\phi-\beta)} e^{j(m-l)} d\beta \tag{10}$$

$$= R_o a_m e^{jm\phi} \left\{ \sum_{p=-\alpha}^{\alpha} [j^m g_p(\theta) J_m(k_o R_o \sin\theta)] \right\} \tag{11}$$

In the above Equation, here J_m is the Bessel function of first kind and $k_o = \left(\frac{2\pi}{\lambda_o}\right)$. Thus, total far field generated by the circular ring array is given by

$$F(\theta,\phi) = \Sigma_\downarrow(m=-\alpha)^\dagger\alpha\boxtimes\square f_1m\,(\theta_1o,\phi)\square\,R_\downarrow o\,\Sigma_\downarrow(m=-\alpha)^\dagger\alpha\boxtimes\square$$
$$a_1m\,e^\uparrow jm\phi\,\square\,\Sigma_\downarrow(p=-\alpha)^\dagger\alpha\boxtimes\square[j^\dagger m\,g_1p\,(\theta)\,J_\downarrow m\,(k_\downarrow o\,R_\downarrow o\,\sin\theta) \tag{12}$$

Each term f_m, in this series is a phase mode for the corresponding phase mode coefficient a_m. These farfield phase modes are omnidirectional in azimuth, however each has phase variation for the corresponding excitation coefficient. From the above equation, it is evident that for a given farfield mode f_m, one can obtain the corresponding phase mode excitation a_m, and aperture excitation $A(\beta)$. So, the entire farfield can be decomposed into individual phase modes as shown in the above equation. At this point, there are two possible types of uniformly spaced discrete arrays which are shown in Figure 2. If the array starts at $\beta = 0$, then $a_m = -a_{m+N}$. However, if the array starts at $= \frac{\beta_o}{2}$, then $a_m = -a_{m+N}$. In either case, from the concept of phase-mode theory, total farfield pattern (θ_o cut) corresponding to the UCA is given by Equation (12).
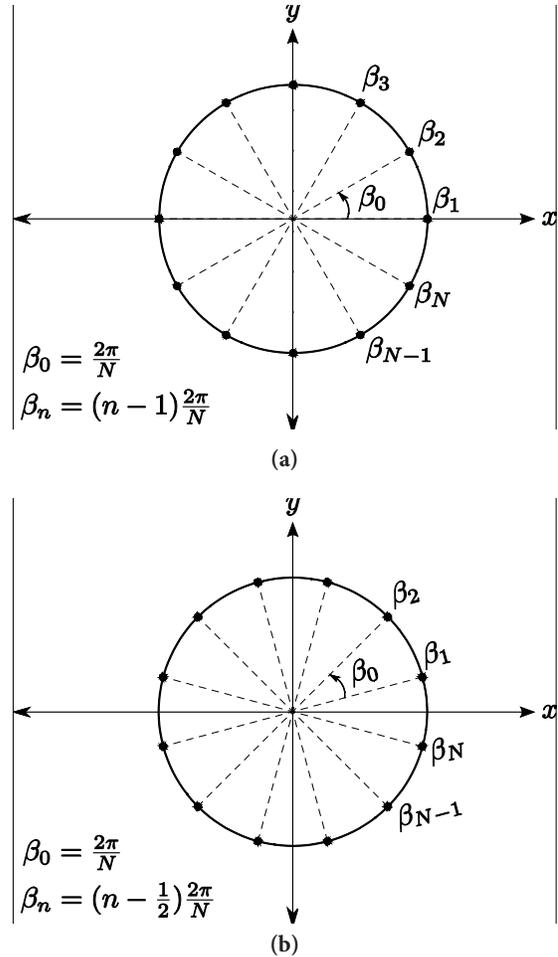

$$\beta_0 = \frac{2\pi}{N}$$
$$\beta_n = (n-1)\frac{2\pi}{N}$$

(a)

$$\beta_0 = \frac{2\pi}{N}$$
$$\beta_n = (n-\tfrac{1}{2})\frac{2\pi}{N}$$

(b)

Figure 2. Uniformly spaced discrete circular ring array. **(a)** Starting at $\beta = 0$. **(b)** Starting at $\beta = \frac{\beta_o}{2}$.

2.2 Isotropic Element Case

For circular array with isotropic element, the weighting of the array elements is corresponding to the sampled continues ring weighting. To generate M spatial harmonics, the number of array elements should be $N > 2\left(\frac{2\pi R}{\lambda}\right) + 1$, for the radius of the circular ring. This implies that the element spacing on the arc is lesser than $\frac{\lambda}{2}$.

For isotropic elements $G_e(\theta,\phi) = 1$, that is

$$g_p(\theta) = \left\{ \begin{matrix} 1 \\ 0 \end{matrix} for\ p = 1\ or\ 0 \right\} \tag{13}$$

For azimuthal plane (i.e., $\theta_o = \frac{\pi}{2}$, the far field pattern is reduced to,

$$F_m(\theta,\phi) = R_o \sum_{m=-\alpha}^{\alpha} a_m j^m J_m(k_o R_o) e^{jm\phi} \tag{14}$$

$$= \sum_{m=-\alpha}^{\alpha} \left(f_m e^{jm\phi} \right) \qquad (15)$$

Where

$$f_m = \frac{1}{2\pi} \int_0^{2\pi} F\left(\frac{\pi}{2}, \phi\right) e^{-jm\phi} d\phi \qquad (16)$$

Which the mode excitation of discrete array can be rewritten as

$$a_m = \frac{f_m}{j^m R_o J_m(k_o R_o)} \qquad (17)$$

While applying these results in Equation (14), it yields well known expression $F = \frac{\sin\left(\frac{N\phi}{2}\right)}{\frac{N\phi}{2}}$. Therefore, the approximate beamwidth is $\frac{2\pi}{N+1}$. This indicates that a large number phase mode (N) can be reducing beamwidth which is analogues to non-uniform excitation or amplitude tapering in linear arrays.

3. Pattern Synthesis: Chebyshev and Zolotarev Weights

Synthesis of Chebyshev and Zolotarev patterns for linear arrays is a well-known concept in antenna literature. However, excitation of Chebyshev patterns for uniform circular ring arrays is rarely reported[25,26]. The systematic development of phase mode excitation with non-uniform weights is difficult process for the desired radiation pattern. To the best knowledge of the authors of this article, there is no paper dealing with synthesis of optimum or near-optimum difference patterns for circular ring arrays. In the present article, authors address this issue too in detail. The goal of synthesis process is to produce a set of complex weights for the circular array, considering directional antenna elements and phase mode excitation, to produce a desired far field D-C or Zolotarev pattern. Initially, for the desired far field Chebyshev/Zolotarev pattern with the desired beam width or Sidelobe Level (SLL) is synthesized. From the calculated Fourier coefficients, A_n, as defined in Equation (2), phase mode excoriations, a_m are calculated using Equation (3). From the set of a_m, we can define the continuous element weight function which represents the amplitude excitation and phase of the current around the array. In summary, pattern synthesis is accomplished by equating the Fourier components of the near and far field phase modes.

3.1 Chebyshev Pattern

Chebyshev patterns can be synthesized using either even or odd order polynomials. In even polynomials, mapping process of farfield is demonstrated by Dolph which had proposed in his classic paper[26]. This can be seen in Figure 3 where an 8th order polynomial is used for mapping. The radiation pattern of an array should have lower near side lobes are required, In addressed the Chebyshev polynomials that devising suitable transformations of variables to link the behavior of the polynomials to array side lobe levels. Chebyshev polynomials oscillate between −1 to +1 in the inner region and then increase in absolute value outside the oscillatory region. Here, the even mode of an array factor is given by;

$$AF = 2\sum_{n=1}^{N} [J_n \cos\left(n-\frac{1}{2}\right)] kd\cos\phi \qquad (18)$$

The polynomials of Chebyshev is given by

$$F_{\downarrow}n\,(x) = \cosh[N\Box\cos\Box^{\uparrow}(-1)\,(x_{\downarrow}o) \qquad (19)$$

For $-1 \leq x \leq +1$ of N even mode, and

$$x_o = \cosh\left[\frac{\cosh^{-1}V_o}{N-1}\right] \qquad (20)$$

The Omni-directional in azimuth (ϕ) in linear array, therefore the CAA excitation coefficients A_n are treated in the same way. So the Dolph Chebyshev (D-C) used to find the magnitude of an element with respect to the phase as usual like LA. In this case the 20 dB SLL with 8 elements array has been carried out with element space angle of d = 0.67λ. If you find the first four order coefficient of excitation, we can apply the same magnitudes to rest of
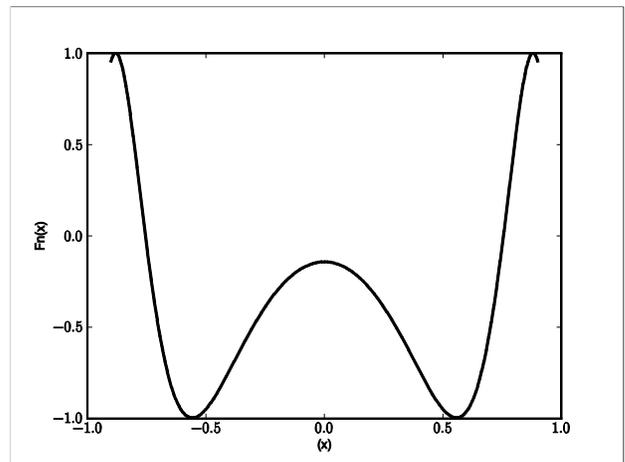

Figure 3. Chebyshev Polynomials of 8th order and corresponding mapping technique.

an element due to symmetry. The orders are calculated by using the Equation (19) using ARRAYTOOL. The array factor can be calculated in terms of x, the calculated in Table 1 with different phase angle. The Dolph Chebyshev weighting techniques of pattern synthesis provide discrete arrays. The Figure 4 shows the array factor equation in terms of order of $F_n(x)$. The amplitude polynomials are responsible for the equal ripple side lobes.

$$F(\phi) = T_n\left[ccos\frac{\phi}{2}\right] \qquad (21)$$

3.2 Zolotarev Pattern

An optimum null pattern is required to have the slope at bore-sight as deep as possible for a given sidelobe level. In[27], Price and Hyneman determined the properties of polynomial for such optimum difference pattern but were not aware of the existence of polynomials possessing these properties. In[28], McNamara used Zolotarev polynomials to achieve such optimum difference patterns. In this article, the same Zolotarev polynomials will be used to obtain optimum null (azimuthal) patterns for circular ring arrays. Since odd polynomials should be used for difference pat-

Table 1. Dolph Chebyshev coefficients for 8 elements array with element spacing d = 0.67 λ

Position of the element (n)	Magnitude (V_n)	Phase angle α_n (deg)
1	$V_1 = 0.308$	$\alpha_1 = 0$
2	$V_2 = 1.9719$	$\alpha_2 = 45$
3	$V_3 = 3.080$	$\alpha_3 = 90$
4	$V_4 = 3.787$	$\alpha_4 = 135$
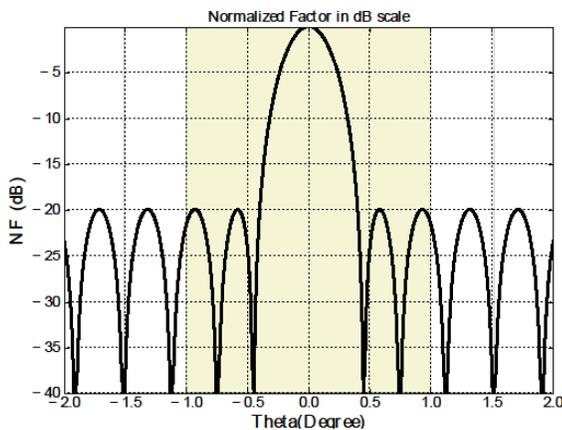
Figure 4. Normalized farfield mode amplitude corresponding to N = 8 and SLL = 20dB.

terns. The polynomial is defined as a hyperbolic cosine of an argument that is N times a function, giving a polynomial of order $2N - 1$. Since the Zolotarev polynomials are less familiar compared to the Chebyshev polynomials, a mapping process which is very similar to Equation (18) should be used as shown in Figure 5. Array factor of the McNamara-Zolotarev difference pattern array is given in terms of the $(M - 1)^{th}$ order Zolotarev polynomial as

$$Af(k_x) = Z_{m-1}\left[csin\left(\frac{k_xd}{2}\right), m\right] \qquad (22)$$

Where,

$$c = csc\left(\frac{k_od}{2}\right) for\ d \le \frac{\lambda}{2}$$

The parameter m is decided by the amount of SLR required. The synthesis procedure will be summarized briefly, for details consult. Given an SLR, and an array of *2N* elements, the order *2N-1* polynomial at the peak is set equal to SLR. The solution of this gives the Jacobi modulus, and the polynomial is completely determined. For half-wave spacing, the polynomial is expanded into a conventional polynomial; from these coefficients the array excitation coefficients may be found. Specific computational details for the special functions are given in the reference above. The mapping relation for optimum difference pattern is given as

$$F(\phi) = Z_p[sin\phi, m] \qquad (23)$$

Once again, substituting Equation (23) into Equation (16) and Equation (3) gives the corresponding continuous aperture distribution. In order to validate the theory proposed in the previous subsections, two synthesis examples are presented for Chebyshev and Zolotarev patterns, respectively. In both the cases, SLR = 20 dB as shown in Figure 6 and order of the mapping polynomial is chosen to be an odd number for ring array synthesis involving even order polynomials etc.
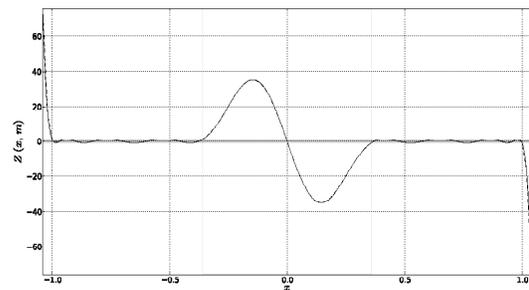
Figure 5. Zolotarev polynomials of even order N = 8 and corresponding mapping F(ϕ).
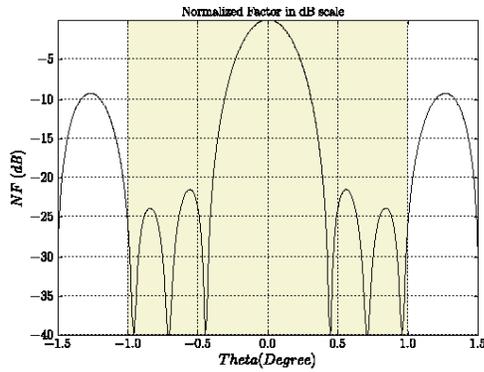
Figure 6. Normalized farfield Zolotarev pattern for N = 8 and SLL = 20 dB.

4. Microstrip Circular Array with Reduced Sidelobe

To illustrate directional elements in micro strip form, the well-known circular and rectangular patch antennas are used in Microstrip Circular Array Antennas (MCAA). Using resonant frequency equation for a single element can be calculated by the excited derivation from, the patches are called elements in circular ring array. The element spacing considering to avoid the mutual coupling between the elements, regarding the radiated phase mode m = 0 represents omnidirectional pattern without amplitude ripple. In this case, we have directional radiating elements, however, and, therefore, higher-order modes will be excited. The interference between the modes causes farfield pattern. The fundamental m = 0 mode, to dominate. For this mode, the J0 kR Bessel function plays an important role. Its first three zeroes and the corresponding element spacing for 8 elements are presented in Table 2. Note that $kR = \dfrac{2d}{\lambda}$. In order to accommodate directional elements into the above development, the element pattern must be transformed into a set of Fourier series coefficients, g_e as shown in Equation (7) and Equation (8). In this the element pattern, in summation form, can be substituted into Equation (6). After simplification, the relation among weight function, element pattern and farfield pattern can then be found by equating the farfield pattern, Equation (2), with the Fourier expansion coefficients in Equation (3) and Equation (5) as:

$$F^{dir} = \sum_m \sum_p \hat{c}_m \frac{1}{2\pi} \int_{-\pi}^{\pi} D_p e^{jp(\phi-\varphi)} e^{jm\phi} e^{jkR_o(\phi-\varphi)} d\varphi$$

$$= \sum_m \sum_p c_m e^{jm\phi} D_p j^{(m-p)} J_{m-p}(kR_o) \qquad (24)$$

Relating to the phase modes c_m in Equation (23) that now include the element pattern Fourier coefficients D_p to the far field phase mode A_m, we arrive at following

$$C_m^{dir} = A_m \left(D_p j^{(m-p)} J_{m-p}(kR_o) \right)^{-1} \qquad (25)$$

All the elements are equally spaced with d = 0.67λ ref Table 2 and operating at 10 GHz with the substrate thickness of h = 0.1588cm and ε_r = 2.2 (RT Duroid 5880). The feed of individual coaxial excitation minimize the mutual coupling between the inter elements. Frequency response and radiation characteristics of individual circular/rectangular patch antenna are shown in Figure 7. Coaxial probes has low spurious radiation pattern. However, it also narrows beamwidth especially for thick substrate (h = 0.02λ_o). The magnitude of DC/Zolotarev coefficients are applied to the micro strip array antennas of circular and rectangular patches. The patches are excited through the coaxial probe with the Chebyshev coefficient. The detailed discussion this circular array is covered in our earlier published reports. Figure 7 shows the circular and rectangular patch arrays in ring (MCAA). Figure 7(c) shows the individual feed by coaxial cables whose phase mode excitations as calculated in Equation (3). Using a 3D simulator (High Frequency Simulation Software), the antenna arrays are simulated at operating frequency to obtain radiation patterns at various azimuthal cuts. Figure 8 shows resulting radiation pattern of DC patch antenna array along with its 3D radiation pattern. From the Figure 9 shows the similar pattern on desired

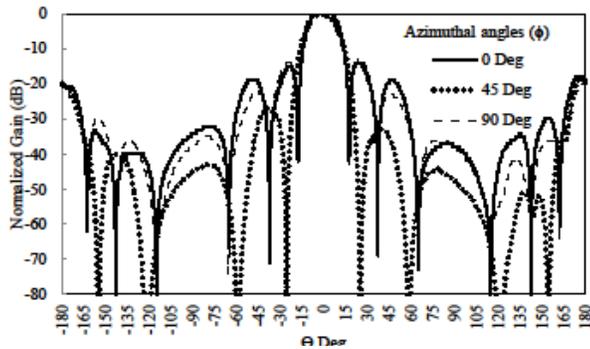**Table 2.** Zeros of J_o(kR) for various combination of d/λ

Zeorth Number	J_n Argument	N=8
1	2.405	d/λ=0.03
2	5.520	d/λ=0.69
3	8.654	d/λ=1.08
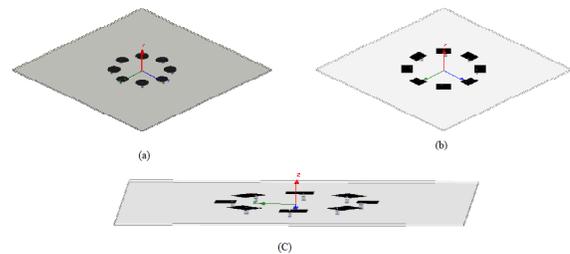
Figure 7. Configuration of. **(a)** Circular. **(b)** Rectangular. **(c)** With coaxial feed.
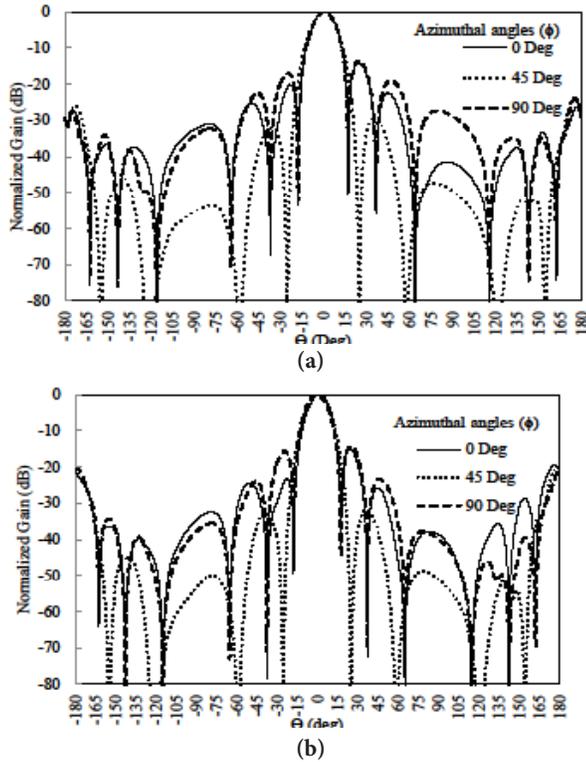
Figure 8. Dolph Chebyshev MCAA of 8 elements. **(a)** Circular. **(b)** Rectangular micro strip antennas with 20dB SLL.

Figure 9. Zolotarev excitation elements in circular ring, the edges of an elements having equal magnitude and desired SLL = 20 dB.

direction. The field distribution of patches is classified in width and length ratio, but in circular patch, the fields can be taken out from the radius. Therefore a very slight difference between these two patches does not affect the total directivity of an array. More over the mutual coupling between the antennas is ☐27dB, which means that excitations are independence each other to propagate in farfield. The normalized gain pattern are shows the major and minor lobes are presented in the radiation pattern

with desired SLL of 20dB, the progressive coefficient of an array has been calculated with Chebyshev and Zolotarev polynomials has discussed. It shows the minimum side-lobe level was formed in between the major lobe or main lobe. The patterns are stable at three different azimuthal angles in the whole elevation angles. The design example of 8 elements with DC amplitude and phase distribution of far field pattern with desired SLL shown in Figure 8 the normalized gain pattern of E and H plane pattern with maximum directivity and the First Null Beamwidth (FNBW) almost same when compared to rectangular array of FNBW = 30dB. But the SLL formed next to the main lobe have slight difference due to field distribution of patch sizes (Width and Length ratio Vs. Radius). The DC excitation with SLL of 20dB, which element spacing $d \geq 1\lambda$ to avoid grating lobes present near to the main lobe $\frac{2\pi}{\lambda_o}$ of visible region. The directional element with DC excitation shows integration of phase/look angles circular array. Similarly the Zolotarev pattern provides equal SLL next to the main lobe with compared to rectangular array, the Figure 9 shows the normalized pattern with FNBW = 30dB. The analytical results of DC and Zolotarev compared with synthesized results, the results of desired SLL have slight changes due to field distribution in edges of both patches MCAA. In Figure 10 illustrates the half of the elements in the ring had the excitation of Chebyshev coefficients, and rest of the elements waveport excitations are equal to zero magnitude or OFF set mode. The center of the elements should give maximum mainlobe at desired azimuthal pattern, the elements in edges of both side have equal ripple magnitude of 1V. The analytical model and Chebyshev models are shown the wider HPBW in a reasonable range.
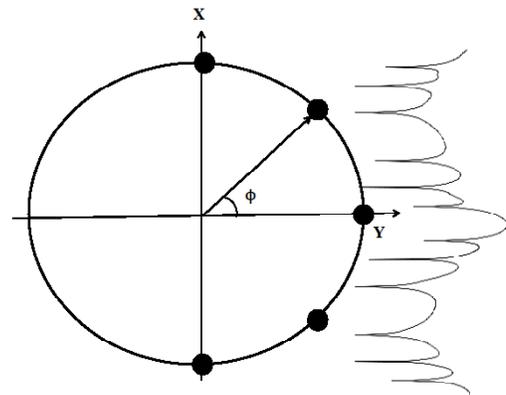
Figure 10. Active elements excitation in MCAA, the edges of elements are having equal magnitude.

5. Conclusion

The pattern analysis and synthesis of circular array theory concept are studied; here the phase mode concepts are useful to the array excitation. The directional elements are excited with well-known Chebyshev and Zolotarev polynomials with even and odd numbers. The radius of CAA depends $kR = \frac{2\pi}{\lambda}$. In order to derive kR, the number of elements should consider. Here commercial 8 elements have been analyzed and the radiation pattern for farfield has plotted by element pattern and array factor equation. The analyzed polynomials of Chebyshev and Zolotarev excitation values are tabled; the coefficients are directly applied to the directional elements. The microstrip patches are arranged in ring manner with the progressive phase, the element pattern of farfield shown the maximum gain with low sidelobe levels. Due to the $\frac{d}{\lambda} = 0.67$ in microstrip patches produced the field around the edges of the patches made the sidelobe levels are very close to the desired side lobe level of 20 dB. The results are valuable and compared with pattern synthesis. The minimum side lobe level of 20 dB exhibit good and it is useful for wireless and RADAR communication.

6. References

1. Fenn AJ, Temme DH, Delaney WP, Courtney WE. The development of phased-array radar technology. Lincoln Laboratory Journal. 2000; 12(2):1–20.
2. Ares F, Mosig JF, Vaccaro S, Vassal'lo J, Moreno E. Satellite communication with moving vehicles on earth: Two prototype circular array antennas. Microwave and Optical Technology Letters. 2003 Oct; 39(1):14–6.
3. Rahim T, Davies D. Effect of directional elements on the directional response of circular antenna arrays. IEE Proceedings H Microwaves, Optics and Antennas. 1982 Feb; 129(1):18–22.
4. Circular array antenna principle for determining azimuth angle of radio transmitter. Available from: http://ieeexplore.ieee.org/document/6146156/
5. Semi-circular antenna array for azimuth DOA estimation. Available from: http://ieeexplore.ieee.org/document/6402959/
6. Chu TS. On the use of uniform circular arrays to obtain omnidirectional patterns. Investigative Reporters and Editors Transactions on Antennas and Propagation. 1959 Oct; 7:436–8.
7. Ram G, Mandal D, Kar R, Ghoshal SP. Design of non-uniform circular antenna arrays using firefly algorithm for side lobe level reduction. International Journal of Electrical, Computer, Electronics and Communication Engineering. 2014; 8(1):36–41.
8. Sector beam forming with uniform circular array antennas using phase mode transformation. Available from: http://ieeexplore.ieee.org/document/6599708/
9. Chatterjee A, Mahanti G. Side lobe reduction of a uniformly excited concentric ring array antenna using evolutionary algorithms. ICTACT Journal on Communication Technology. 2010 Sep; 1:230–4.
10. Balanis CA. Antenna theory: Analysis and design. 3rd ed. New Jersey: John Wiley and Sons; 2005.
11. Knudsen HL. The field radiated by a ring quasi-array of an infinite number of tangential or radial dipoles. Investigative Reporters and Editors Proceedings. 1953 Jun; 41(6):781–9.
12. Knudsen HL. Radiation resistance and gain of homogeneous ring quasi-array. Investigative Reporters and Editors Proceedings. 1954 Apr; 42(4):686–95.
13. Knudsen HL. Radiation from ring quasi-arrays. IRE Transactions on Antennas and Propagation. 1956 Jul; 4(3):452–72.
14. Rahim T, Davies D. Effect of directional elements on the directional response of circular antenna arrays. IEE Proceedings H Microwaves, Optics and Antennas. 1982 Feb; 129(1):18–22.
15. Rahim T. Analysis of the element pattern shape for circular arrays. Electronics Letters. 1983 Sep; 19(20):838–40.
16. Josefsson L, Persson P. Conformal array antenna theory and design. New Jersy: John Wiley; 2006.
17. Davies D. A transformation between the phasing techniques required for linear and circular aerial arrays. Proceedings of the Institution of Electrical Engineers. 1965 Nov; 112(11):2041–5.
18. Malathi ACJ, Mohan KN. Effect of discretization on the azimuthal pattern of circular ring array. International Journal of Applied Engineering Research. 2014; 9(21):9365–74.
19. Design and analysis of linear, planar, circular array using Arraytool. Available from: https://www.researchgate.net/publication/275894160_Design_and_analysis_of_linear_planar_and_circular_array_using_ARRAY_TOOL
20. Arraytool: An open source python based package for array antenna analysis and design. Available from: https://zinka.wordpress.com/tag/srinivasa-rao-zinka/
21. Fenby RG. Limitations on directional patterns of phase-compensated circular arrays. Radio and Electronic Engineer. 1965 Oct; 30(4):206–22.
22. James PW. Polar patterns of phase-corrected circular arrays. Proceedings of the Institution of Electrical Engineers. 1965 Oct; 112:1839–48.
23. Villeneuve A. Taylor patterns for discrete arrays. IEEE Transactions on Antennas and Propagation. 1984 Oct; 32:1089–93.
24. A dolph-chebyshev approach to the synthesis of array patterns for uniform circular arrays. Available from: http://ieeexplore.ieee.org/document/857042/

25. Null control for linear arrays by phase-only or amplitude only modification of the excitations, Available from: http://ieeexplore.ieee.org/document/788363/

26. Dolph C. A current distribution for broadside arrays which optimizes the relationship between beam width and side-lobe level. Proceedings of the Investigative Reporters and Editors. 1946 Jun; 34(6):335–48.

27. Price O, Hyneman R. Distribution functions for mono pulse antenna difference patterns. IRE Transactions on Antennas and Propagation. 1960 Dec; 8(6):567–76.

28. McNamara DA. Direct synthesis of optimum difference patterns for discrete linear arrays using Zolotarev distributions. IEE Proceedings of Microwaves, Antennas and Propagation. 1993 Dec; 140(6):495–500.